J. Chem. Thermodynamics **1999,** 31, 55–69
Article No. jcht.1998.0415
Available online at http://www.idealibrary.com on IDEAL

JCT

The speed of sound and isentropic compressibility of liquid difluoromethane (HFC32) from $T = (248$ to 343) K and pressures up to 65 MPa

P. F. Pires and H. J. R. Guedes[a]

Departamento de Química, Centro de Química Fina e Biotecnologia, Faculdade de Ciências e Tecnologia, Universidade Nova de Lisboa, P-2825 Monte de Caparica, Portugal

This work reports experimental data on the speed of sound in liquid difluoromethane (HFC32, or R32) from $T = (248$ to 343) K and pressures up to 65 MPa. The results were obtained using a newly-built apparatus, calibrated with toluene over the whole experimental region, and show good agreement with two available data sets. The uncertainties are ± 0.01 K in the temperature, ± 0.025 MPa in the pressure up to 35 MPa, and ± 0.2 MPa above this value. The final uncertainty on the speed of sound is estimated to be ± 0.2 per cent. The data were fitted using a simple analytical equation and the results are discussed. The isentropic compressibility was calculated over the (p, T) surface where the reported speed of sound values and the corresponding literature densities overlap. © 1999 Academic Press

KEYWORDS: speed of sound; alternative refrigerants; difluoromethane; HFC32; isentropic compressibility

1. Introduction

International agreements, such as the 1987 Montreal Protocol on Substances that Deplete the Ozone Layer in the stratosphere, and its 1990 London Amendment,[1] called for the elimination of chlorofluorocarbons (CFCs). Subsequently, hydrochlorofluorocarbons (HCFCs) were added to the list of substances to be phased out, both at the 1993 Montreal Protocol[2] and, recently, at the 7th Meeting of the Parties to the Montreal Protocol, held in Vienna, 1995.[3] However, it has been recognized that more work regarding the replacement of both CFCs and HCFCs needs to be done.[4]

Reliable information on the thermophysical properties of alternative refrigerants, or refrigerant mixtures plays an essential role not only in identifying the most promising candidates likely to replace conventional refrigerants, but also in designing and manufacturing environmentally acceptable equipment for handling

[a] To whom correspondence should be addressed (E-mail: h.guedes@dq.fct.unl.pt).

0021–9614/99/010055 + 15 $30.00/0

the new alternatives.[5] In addition to (vapour + liquid) equilibria (VLE) and (p, V_m, T), or (p, V_m, T, x) data for the case of mixtures, it is also essential to have experimental data on other thermodynamic properties, such as heat capacities and speeds of sound.[3]

Difluoromethane (HFC32) is an ozone-friendly refrigerant which, whether used pure, or as a major component in refrigerant blends, is a good substitute for chlorodifluoromethane (HCFC22) and the azeotropic blend HCFC502 {of mass fraction composition (0.488 $CHClF_2$ + 0.512 $CClF_2CF_3$)} in low-temperature refrigeration, air conditioning, and heat pump applications. As HFC32 does not contain chlorine atoms, its ozone depletion potential is nil. Its global warming potential is less than that of HCFC22 because of its shorter atmospheric lifetime due to its higher content of hydrogen atoms. Owing to its importance, there is a broad interest in the knowledge of its thermophysical properties which have been the object of several experimental studies. Several theoretical and semi-empirical studies have been performed, such as computer simulation,[6] perturbation theories,[7] and corresponding states model.[8–10]

In the present work we report values of the speed of sound u of HFC32. The results cover a larger (p, T) surface than the surfaces previously investigated, with temperatures ranging from T = (248 to 343) K and pressures up to 65 MPa. The data are compared with those of other authors.[11–13] The isentropic compressibilities are also calculated using the available literature density values.

2. Experimental

In order to measure the ultrasonic speed of sound with a high accuracy in the temperature range (240 to 370) K and pressures up to 65 MPa, a cell based on the pulse-echo method adapted from Papadakis[14] and Guedes and Zollweg[15] {figure 1(a)} was designed and built. The cell is made up of a piezoelectric transducer and a structure that provides mechanical support and also minimizes the interferences caused by the diffraction of sound waves. The transducer is a small disc made of a polarized piezoelectric ceramic of lead–titanate–zirconate ($PbZrO_3/PbTiO_3$) and gold-plated on both faces. The deposited metal serves as an electrode. One of the faces is in contact with a copper ring, partially insulated with Teflon. The transducer, with a mass of 2.0485 g, 12.5 mm in diameter and of 2.1 mm thickness, operates at its fundamental resonance frequency of 1 MHz. Both the transducer and the copper ring are held together between two stainless-steel pieces. The acoustic cell includes two steel reflectors kept at unequal distances from the transducer by two sets of copper spacers. The lengths of these spacers are (45 and 25) mm at room temperature and ambient pressure, and are made from a 4.8 mm diameter copper rod. The copper used is of high purity (mass fraction = 0.9999), which allows the accurate prediction of both its thermal expansion and compressibility behaviour in the whole range of pressure and temperature.

To support the high pressure, a stainless-steel cylinder {figure 1(b)} was built with 50 mm internal diameter and 15 mm wall thickness. A Bridgman unsupported area seal was made by extrusion of a Teflon ring between a piston and the cylinder

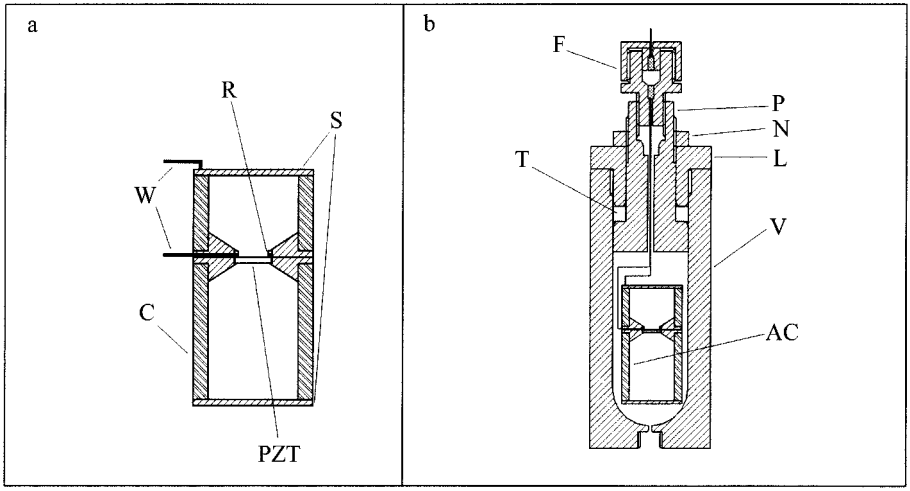

FIGURE 1. Schematic diagram of: a, the acoustic cell; and b, the pressure vessel. PZT, piezoelectric transducer; C, copper spacers; S, steel reflectors; R, partially insulated copper ring; W, conducting wires; F, electrical feedthrough; T, Teflon sealing o-ring; P, piston; N, nut; L, closure; V, pressure vessel; AC, acoustic cell.

closure. The electrical connections needed were provided by an electrical feed-through designed for high pressures. The total volume of the cell is about 150 cm^3.

The rest of the apparatus (figure 2) was built using standard high-pressure valves, tubing, and other equipment. The apparatus includes a vacuum pump and a piston pressure intensifier of 30 cm^3, equipped with Teflon sealing o-rings, capable of reaching pressures of about 70 MPa. The pressure intensifier can be cooled with an ice-bath, if needed.

A Setra Systems Inc. transducer was used to measure the pressure for the lower pressure range (up to $p = 35$ MPa), and a Digibar transducer for the higher pressure range (up to $p = 200$ MPa). The pressure sensors were calibrated and the pressure could be measured with an uncertainty of ± 0.025 MPa in the lower range, and ± 0.2 MPa in the higher range.

The acoustic cell was thermostatted inside a Dewar by means of both constant cooling and heat pulses provided by an electrical resistance heater and a p.i.d. controller. The temperature was measured by a platinum resistance thermometer and a digital multimeter of six and a half digits, and was stable to within ± 0.01 K. The thermometer was previously calibrated, thus allowing temperature measurements with an uncertainty of ± 0.01 K, on ITS 90.

To measure the ultrasonic speed of sound, we used a synthesizer (figure 3) to generate a burst of five cycles with a frequency of 1 MHz and amplitude of 15 V peak-to-peak. This signal was fed to the piezoelectric transducer. The response signal was collected through the same wire, amplified, and then passed through a band-pass filter with an overall voltage gain of about 35 dB at the frequency of 1 MHz. The filtered signal was observed in a digital oscilloscope.

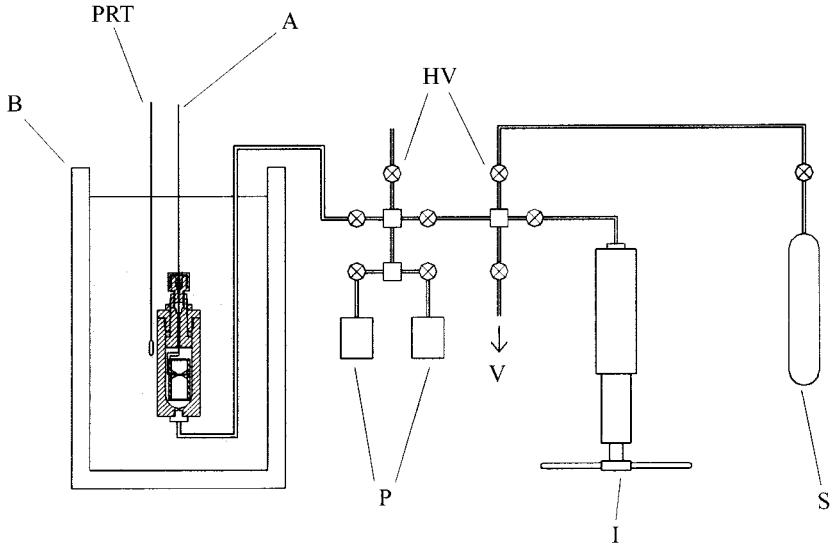

FIGURE 2. Schematic diagram of the apparatus for the measurement of the speed of sound of liquids at high pressures. B, thermostatted bath; PRT, platinum resistance thermometer; A, acoustic signal lead; HV, high pressure valves; P, pressure transducers; I, piston pressure intensifier; S, HFC32 sample cylinder.

When a sinusoidal pulse excites the piezoelectric transducer it generates two acoustic waves which propagate in opposite directions, each one hitting a reflector and thus producing two sets of echoes. Using an oscilloscope we can then measure the time interval between the first of each set of echoes and calculate the speed of sound u, using the following equations:

$$u = \theta(p,T)/\delta t, \tag{1}$$

$$\theta(p,T) = 2(d_1 - d_2), \tag{2}$$

where $\theta(p,T)$ is the parameter that relates the speed of sound u with δt, the time

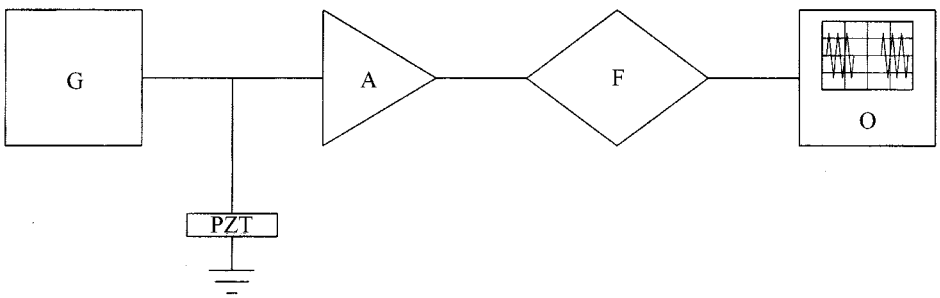

FIGURE 3. Electrical schematic of the apparatus for the measurement of the speed of sound of liquids at high pressures. G, 1 MHz pulse generator; PZT, piezoelectric transducer; A, signal amplifier; F, 1 MHz band-pass filter; O, digital oscilloscope.

interval between the two first sets of echoes of each reflector, and d_1 and d_2 are the distances between the piezoelectric transducer and the reflectors. These values depend both on the pressure p and the temperature T of the system, and can be evaluated by measuring the speed of sound of a reference substance at $T = 298.15\,\mathrm{K}$ and $p = 0.1\,\mathrm{MPa}$. The change in the path length caused by the thermal expansion and compressibility of the copper spacers can also be calculated.

Another method of calibrating the acoustic cell path length is to measure the time intervals for a known substance in the whole experimental range, calculate the u times δt, and then fit the data to an equation. We used the latter method. We calibrated the cell with toluene and compared our results with literature u data.[16] Finally, we fitted our results to the following equation:

$$\theta(p,T)/(10^{-6}\,\mathrm{m}) = 3.3372\cdot10^{-2} + 1.944\cdot10^{-6}p/(\mathrm{MPa}) + 7.7344\cdot10^{-2}/T(\mathrm{K}). \tag{3}$$

The two calibration methods give similar results, with the values of $\theta(p,T)$ at the extreme conditions of pressure and temperature varying by less than ±0.2 per cent.

The uncertainty in the measurement of δt is $\pm2\cdot10^{-9}\,\mathrm{s}$ and contributes an uncertainty of $\pm0.03\,\mathrm{m\cdot s^{-1}}$ to u, *i.e.* less than ±0.01 per cent.

The HFC32 used was supplied by ICI with a mass fraction purity of 0.998. Further purification consisted of a degassing (freezing the sample in liquid nitrogen followed by vacuum degassing) operation. This procedure was repeated at least three times. Finally the sample was dried with molecular sieves. The same sample was used by other workers[17] for dielectric constant measurements.

3. Results and discussion

Using the apparatus described above, we measured 305 values of the speed of sound of the alternative refrigerant HFC32 (difluoromethane) along ten isotherms in the temperature range (248 to 343) K and at pressures up to 65 MPa.

The (p,T) region covered by the present measurements, and the measurements of the speed of sound[11–13] and density[18] available in the literature is shown in figure 4. Our results are shown both in figure 5 and in table 1. A few data values were randomly repeated, allowing us to estimate a precision of $\pm0.4\,\mathrm{m\cdot s^{-1}}$ for the measurements.

We have examined several equations for fitting the experimental data. The best results were obtained with the equation in which the speed of sound u was expressed as a function of the reduced pressure $p_\mathrm{r} = (p/p_\mathrm{c})$ and the reduced temperature $T_\mathrm{r} = (T/T_\mathrm{c})$,

$$\begin{aligned} u &= \alpha(T_\mathrm{r}) + \beta(T_\mathrm{r})\cdot\ln\{p_\mathrm{r}(+\gamma)T_\mathrm{r}\}, \\ \alpha(T_\mathrm{r}) &= a_0 + a_1T_\mathrm{r} + a_2T_\mathrm{r}^2, \\ \beta(T_\mathrm{r}) &= b_0 + b_1T_\mathrm{r} + b_2T_\mathrm{r}^2, \\ \gamma(T_\mathrm{r}) &= c_0 + c_1/T_\mathrm{r}. \end{aligned} \tag{4}$$

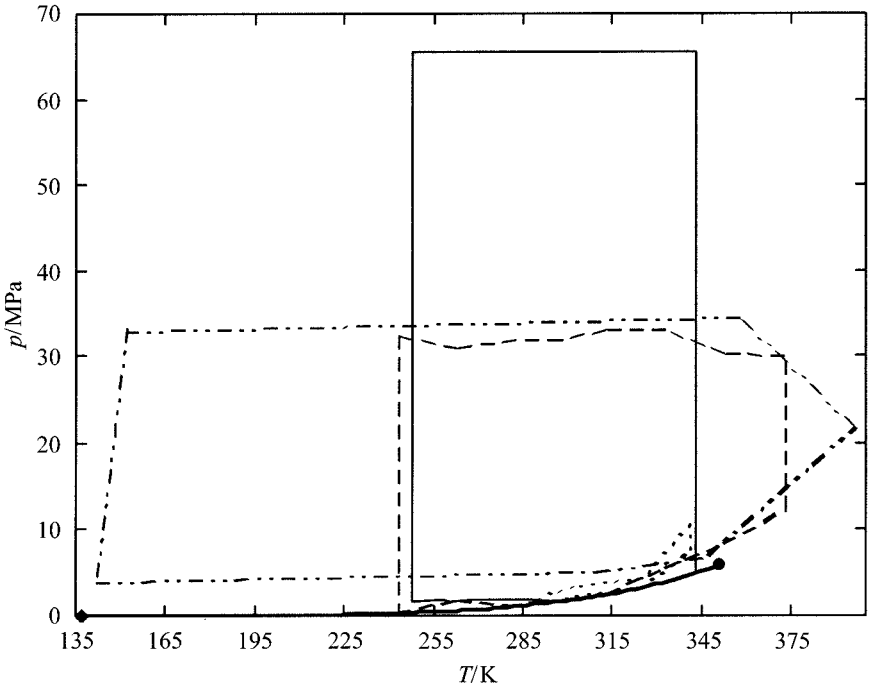

FIGURE 4. Pressure–temperature regions covered by different investigators: ———, this work (u, p, T); - - - -, Takagi (u, p, T); ·····, Grebenkov (u, p, T); – · · – · , Magee (p, V, T); ♦, triple point; ●, critical point; ———, saturation line.

The standard deviation of the fit was $3.5\,\mathrm{m\cdot s^{-1}}$, as shown in table 2 (fit A, table 3). However, larger deviations occurred in the near critical region, *i.e.* above $T = 316\,\mathrm{K}$ ($T_\mathrm{r} = 0.9$) and below 17 MPa ($p_\mathrm{r} = 3$).

To test the consistency of our experimental results, we have fitted equation (4) to some restricted areas of the (u, p, T) surface. By excluding the near critical region results, the standard deviation was reduced to $1.5\,\mathrm{m\cdot s^{-1}}$ (fit B, table 2). By considering only the low density region, the resulting standard deviation of the fit was $2.1\,\mathrm{m\cdot s^{-1}}$ (fit C, table 3). We believe this is due to both the difficulty of fitting a simple analytical equation including all the data, and to the larger experimental errors near the critical point. In fact, in this region the sound absorption increases and, consequently, the diminished amplitude and the distorted shape of the echoes increase the uncertainty of the measurements.

We have also checked the individual isotherms, having observed standard deviations always better than $0.4\,\mathrm{m\cdot s^{-1}}$, except at the $T = 343\,\mathrm{K}$ isotherm. Again, larger deviations occurred at speeds of sound below $500\,\mathrm{m\cdot s^{-1}}$.

In order to compare our experimental results with those of Takagi,[11] we fitted the data above $u = 450\,\mathrm{m\cdot s^{-1}}$ and below $p = 35\,\mathrm{MPa}$ with a standard deviation of $1.0\,\mathrm{m\cdot s^{-1}}$ (fit D, table 2), that is on the whole below ± 0.2 per cent, as can be seen in figure 6. The deviations of Takagi's experimental data,[11] as well as those of

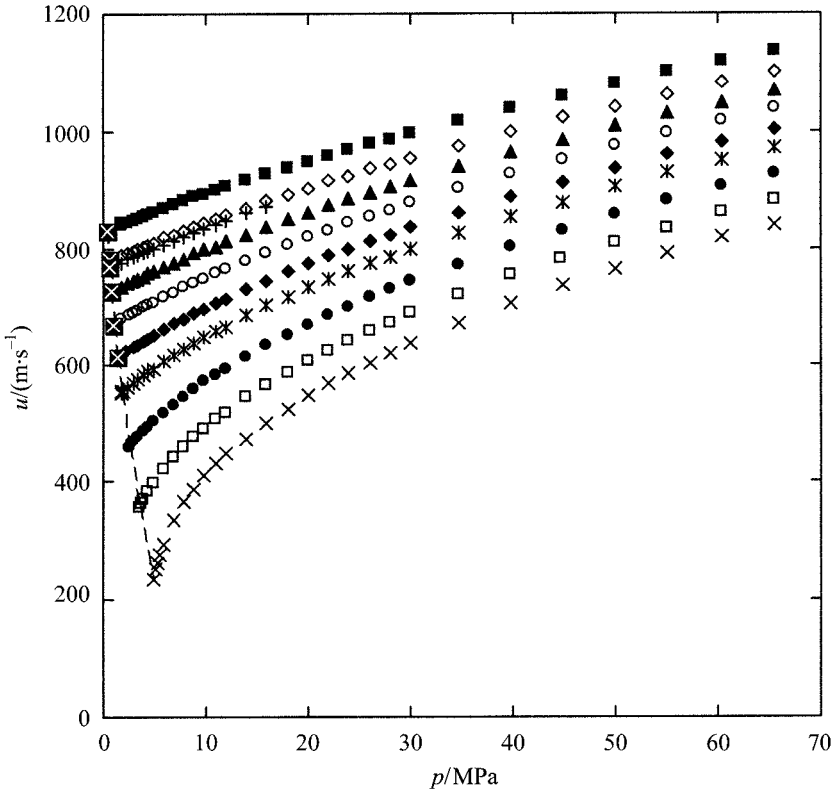

FIGURE 5. Pressure p dependence of the speed of sound u of HFC32 at different temperatures T: ■, $T = 248.20$ K; ◇, $T = 258.13$ K; +, $T = 260.80$ K; ▲, $T = 268.22$ K; ○, $T = 278.12$ K; ◆, $T = 288.31$ K; ✳, $T = 298.18$ K; ●, $T = 313.19$ K; □, $T = 328.15$ K; ×, $T = 343.29$ K; ⊠, extrapolated; ———, saturation line.

Grebenkov and colleagues[12–13] from our fit are shown in figure 7. Above $p = 35$ MPa the deviations are smaller than $\pm 0.6\ \mathrm{m \cdot s^{-1}}$ (fit E, table 2).

In the (p, T) region of greater industrial relevance, *i.e.* from the saturation pressure to $p = 10$ MPa and below $T = 320$ K ($T_r < 0.9$), our experimental data can be fitted with a standard deviation less than $0.7\ \mathrm{m \cdot s^{-1}}$ (fit F, table 2).

Table 4 shows the speed of sound u_σ of the saturated liquid HFC32 along our experimental temperatures. These values were fitted with a standard deviation less than 0.25 per cent, except above $T = 320$ K ($T_r > 0.9$), to a third order polynomial {equation (5)}:

$$u_\sigma/(\mathrm{m \cdot s^{-1}}) = 4132.66 - 28.5782 \cdot (T/\mathrm{K}) + 0.091373 \cdot (T/\mathrm{K})^2 - 0.000119982 \cdot (T/\mathrm{K})^3. \quad (5)$$

The experimental data are plotted in figure 8, together with the extrapolated values of Takagi,[11] which agree within $\pm 1.0\ \mathrm{m \cdot s^{-1}}$ with our data.

4. Calculation of isentropic compressibilities

Using our speed of sound data together with the (p, ρ, T) data of Magee,[18] we have calculated the isentropic compressibilities within the temperature range (250 to 340) K and at pressures ranging from the vapour pressures up to $p = 35$ MPa.

TABLE 1. Experimental data of the speed of sound u of HFC32 at temperatures from $T = 248$ K to $T = 343$ K and pressures p up to 65 MPa

p/MPa	u/(m·s^{-1})	p/MPa	u/(m·s^{-1})	p/MPa	u/(m·s^{-1})	p/MPa	u/(m·s^{-1})
			$T = 248.20$ K				
1.74	842.8	4.90	863.2	13.93	916.4	29.98	997.5
1.82	843.6	5.90	869.1	15.94	926.9	34.65	1016.7
1.83	843.5	6.90	875.3	17.96	938.4	39.81	1038.1
2.36	846.5	7.90	881.7	19.97	948.1	44.97	1059.6
2.91	849.8	8.90	888.0	21.98	959.2	50.03	1078.2
3.41	853.4	9.90	893.2	23.99	969.3	55.19	1098.4
3.90	856.8	10.91	899.0	26.00	978.0	60.35	1117.0
4.40	860.1	11.91	905.3	28.00	987.8	65.42	1133.6
			$T = 258.13$ K				
1.79	789.2	6.90	825.1	17.96	893.2	34.65	976.7
2.36	793.7	7.90	832.3	19.97	904.6	39.81	1000.9
2.91	797.5	8.90	839.2	21.98	915.5	44.97	1022.8
3.41	801.0	9.90	845.1	23.99	925.6	50.03	1042.7
3.90	804.6	10.91	851.5	26.00	936.5	55.19	1063.6
4.40	808.1	11.91	858.2	28.00	946.0	60.35	1081.7
4.90	811.7	13.93	869.9	29.98	956.0	65.42	1100.1
5.90	819.0	15.94	882.3				
			$T = 260.80$ K				
1.74	777.2	3.90	793.5	6.90	814.6	10.91	841.4
2.33	781.3	4.40	796.9	7.90	821.4	11.91	847.5
2.91	785.5	4.90	800.3	8.90	828.2	13.93	860.4
3.41	789.4	5.90	806.9	9.90	835.0	15.94	871.8
			$T = 268.22$ K				
1.77	735.6	5.90	768.7	15.94	838.1	34.65	940.8
2.36	740.7	6.90	776.8	17.96	850.1	39.81	965.1
2.91	745.0	7.90	783.5	19.97	862.4	44.97	987.3
3.41	749.0	8.90	791.4	21.98	874.1	50.03	1008.8
3.90	753.3	9.90	798.3	23.99	885.5	55.19	1029.9
4.40	757.3	10.91	805.1	26.00	896.5	60.35	1049.4
4.90	761.2	11.91	812.3	28.00	907.6	65.42	1068.7
4.90	761.1	13.93	825.3	29.98	917.3		
			$T = 278.12$ K				
1.79	678.7	6.90	724.9	15.94	793.1	34.65	901.8
2.45	684.9	7.90	733.3	17.96	806.4	39.81	928.1
2.91	689.6	8.90	741.5	19.97	819.1	44.97	951.9
3.41	694.2	9.90	749.2	21.98	832.2	50.03	974.7
3.90	698.7	10.91	757.5	23.99	843.6	55.19	996.4
4.40	703.4	10.91	757.2	26.00	855.7	60.35	1017.3
4.90	707.7	11.91	764.4	28.00	866.6	65.42	1036.6
5.90	716.3	13.93	779.0	29.98	877.9		

TABLE 1—*continued*

p/MPa	u/(m·s^{-1})	p/MPa	u/(m·s^{-1})	p/MPa	u/(m·s^{-1})	p/MPa	u/(m·s^{-1})
			T = 288.31 K				
1.77	617.1	5.90	661.5	17.96	760.9	44.97	914.9
1.78	617.2	6.90	670.8	19.97	775.2	50.03	939.1
2.23	622.5	7.90	680.3	21.98	788.7	50.03	939.0
2.23	622.4	8.90	689.7	23.99	801.4	55.19	962.8
2.91	629.9	9.90	698.2	26.00	814.2	55.19	963.1
3.41	635.8	10.91	707.1	28.00	825.7	60.35	984.2
3.90	641.0	11.91	715.2	29.98	837.8	65.42	1003.9
4.40	646.3	13.93	731.0	34.65	863.5		
4.90	651.3	15.94	746.3	39.81	889.7		
			T = 298.18 K				
1.69	552.7	4.90	594.4	13.93	684.6	29.98	799.5
1.71	553.0	5.90	606.2	15.94	701.9	34.65	826.9
1.76	553.7	6.90	617.7	17.96	717.6	39.81	855.0
1.92	555.9	7.90	627.7	19.97	732.8	44.97	881.0
2.41	562.8	8.90	638.1	21.98	747.7	50.03	905.9
2.91	569.5	9.90	648.6	23.99	761.0	55.19	929.0
3.41	576.2	9.90	648.5	26.00	774.4	60.35	953.0
3.90	582.6	10.91	658.0	28.00	787.0	65.42	973.7
4.40	588.9	11.91	667.0				
			T = 313.19 K				
2.49	459.2	6.90	532.7	21.98	685.5	34.65	772.2
2.49	459.2	7.90	546.2	23.99	700.9	39.81	802.7
2.49	458.4	8.90	558.8	26.00	715.6	44.97	831.9
2.49	458.3	9.90	571.1	28.00	729.6	44.97	831.5
2.75	464.5	10.91	582.8	29.98	743.1	50.03	857.3
2.91	467.7	11.91	593.3	29.98	743.1	55.19	881.8
3.41	476.7	13.93	614.4	29.98	743.4	55.19	882.1
3.90	486.3	15.94	633.7	29.98	743.1	60.35	905.3
4.40	494.5	17.96	651.9	29.98	743.2	60.35	905.7
4.90	502.7	19.97	668.9	34.65	772.6	65.42	927.8
5.90	517.9	21.98	685.5				
			T = 328.25 K				
3.54	356.3	7.90	458.3	17.96	587.6	34.76	720.0
3.68	360.8	8.90	475.1	19.97	606.7	39.80	753.5
3.90	368.0	9.90	488.4	21.98	625.0	44.79	781.3
4.40	382.2	10.91	505.4	23.99	642.3	50.05	810.1
4.90	395.7	11.91	518.5	26.00	658.6	55.19	836.1
5.90	419.5	13.93	543.4	28.00	674.0	60.35	861.0
6.90	439.8	15.94	566.4	29.98	688.6	65.42	883.9
			T = 343.29 K				
4.96	235.8	8.90	385.1	19.97	546.6	39.81	705.7
5.12	251.1	9.90	411.7	21.98	567.3	44.97	738.0
5.22	261.2	10.91	431.3	23.99	586.2	50.03	766.2
5.45	276.3	11.91	448.6	26.00	603.8	55.09	793.5
5.90	294.6	13.93	472.7	28.00	621.1	60.35	819.4
6.90	335.1	15.94	499.8	29.98	637.0	65.42	842.8
7.90	364.9	17.96	524.9	34.65	671.1		

TABLE 2. (u, p, T) surface regions where data are fitted to equation (4). u is the speed of sound, p is the pressure, T is the temperature, and σ is the standard deviation of the fit

Fit	range			$\sigma/(\mathrm{m\cdot s^{-1}})$
	p/MPa	T/K	$u/(\mathrm{m\cdot s^{-1}})$	
A	*	248–343	all data	3.5
B	*	248–343	>500	1.5
C	*	248–343	<500	2.1
D	<35	248–343	>450	1.0
E	>35	248–343	*	0.6
F	<10	248–343	*	0.7

* No restrictions were applied.

Using fit D from table 2, we have calculated the speed of sound at rounded values of p at each temperature. The experimental values of the density were fitted to the equation:

$$\begin{aligned} \rho &= \alpha(T) + \beta(T)\cdot\ln\{p + \gamma(T)\}, \\ \alpha(T) &= a_0 + a_1 T + a_2 T^2, \\ \beta(T) &= b_0 + b_1 T + b_2 T^2, \\ \gamma(T) &= c_0 + c_1/T, \end{aligned} \tag{6}$$

TABLE 3. Coefficients a_i, b_i, and c_i for the various fits to equation (4). $T_c = 351.35$ K and $p_c = 5.795$ MPa[19]

Fit	i	a_i	b_i	c_i
A	0	$2.53511\cdot10^{+1}$	$1.12322\cdot10^{+2}$	$-2.60422\cdot10^{+1}$
	1	$-1.22451\cdot10^{+3}$	$1.13053\cdot10^{+3}$	$2.56473\cdot10^{+1}$
	2	$1.47839\cdot10^{+3}$	$-1.02196\cdot10^{+3}$	
B	0	$4.25824\cdot10^{+2}$	$1.69992\cdot10^{+2}$	$-2.13412\cdot10^{+1}$
	1	$-1.59111\cdot10^{+3}$	$7.88886\cdot10^{+2}$	$2.20418\cdot10^{+1}$
	2	$1.27531\cdot10^{+3}$	$-6.74917\cdot10^{+2}$	
C	0	$2.94764\cdot10^{+3}$	$-1.37735\cdot10^{+3}$	$-1.68099\cdot10^{+1}$
	1	$-5.46198\cdot10^{+3}$	$3.74664\cdot10^{+3}$	$1.59243\cdot10^{+1}$
	2	$2.90825\cdot10^{+3}$	$-2.24834\cdot10^{+3}$	
D	0	$9.11125\cdot10^{+1}$	$2.19309\cdot10^{+2}$	$-2.21622\cdot10^{+1}$
	1	$-5.05584\cdot10^{+2}$	$6.51167\cdot10^{+2}$	$2.16690\cdot10^{+1}$
	2	$7.13384\cdot10^{+2}$	$-6.68200\cdot10^{+2}$	
E	0	$-1.50890\cdot10^{+3}$	$5.59377\cdot10^{+2}$	$-3.12820\cdot10^{+1}$
	1	$7.39347\cdot10^{+2}$	$4.00925\cdot10^{+2}$	$3.34590\cdot10^{+1}$
	2	$6.83642\cdot10^{+2}$	$-6.11386\cdot10^{+2}$	
F	0	$-3.37448\cdot10^{0}$	$1.53229\cdot10^{+2}$	$-2.23565\cdot10^{+1}$
	1	$-5.26376\cdot10^{+1}$	$8.12028\cdot10^{+2}$	$2.12426\cdot10^{+1}$
	2	$4.65040\cdot10^{+2}$	$-8.29947\cdot10^{+2}$	

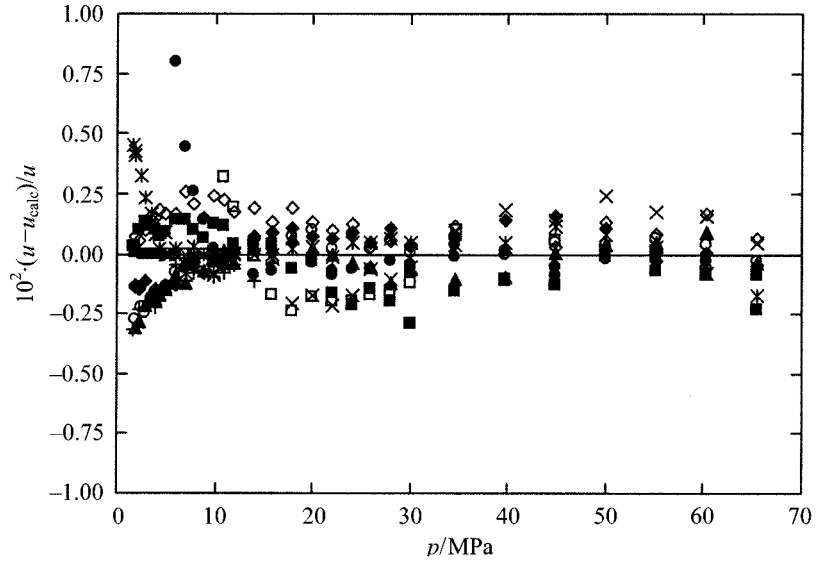

FIGURE 6. Per cent deviations of the speed of sound u from values calculated from equation (4) at different temperatures T: ■, T = 248.20 K; ◇, T = 258.13 K; +, T = 260.80 K; ▲, T = 268.22 K; ○, T = 278.12 K; ◆, T = 288.31 K; ✳, T = 298.18 K; ●, T = 313.19 K; □, T = 328.25 K; ×, T = 343.29 K.

with a standard deviation of 2.3 kg·m^{-3}. The resulting parameters of this equation are shown in table 5.

The isothermal compressibility was calculated from equation (7) at rounded values of p and T using,

$$\kappa_s = \left(\rho \cdot u^2\right)^{-1}, \tag{7}$$

and the isotherms are presented in figure 9.

5. Conclusions

The newly-built apparatus allows the measurement of the speed of sound of liquids over a broad range of temperatures and at pressures ranging from the vapour pressure up to p = 65 MPa with a high accuracy. It was tested with a widely studied alternative refrigerant, HFC32, and the results show good agreement with the data reported by other authors. The experimental pressure range was extended to p = 65 MPa, and the speed of sound of the saturated liquid was determined up to T_r = 0.977. The isentropic compressibility was calculated within the experimental range where density data were available, *i.e.* up to p = 35 MPa.

It is hoped that the exhaustive set of data reported here will contribute to the

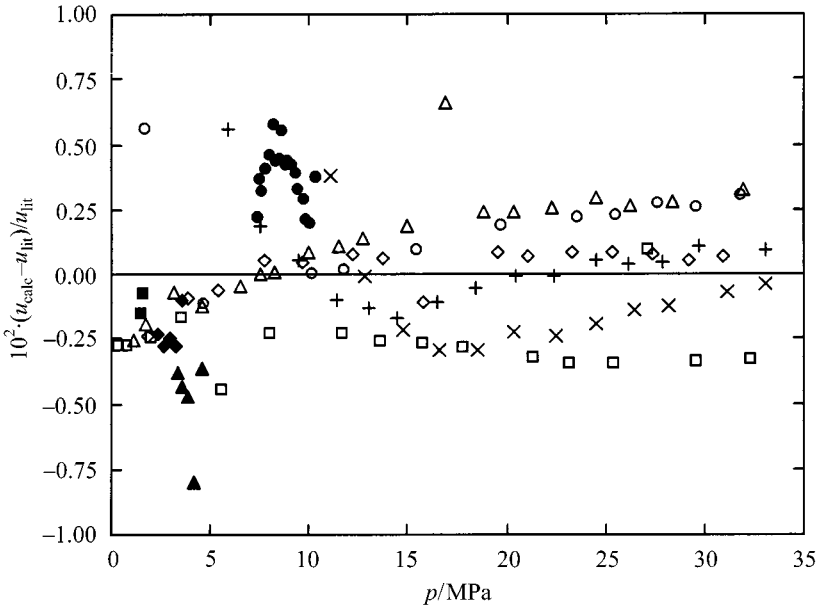

FIGURE 7. Per cent deviations of the literature speed of sound u_{lit} from values calculated using equation (4) u_{calc}. Filled symbols refer to the data of Grebenkov *et al.*,[12,13] and open symbols to the data from Takagi.[12] Temperature: □, T = 243.15 K; ◇, T = 263.15 K; △, T = 283.15 K; ○, T = 298.15 K; +, T = 343.15 K; ×, T = 333.15 K; ■, T = 286.85 K; ◆, T = 302.36 K; ▲, T = 325.93 K; ●, T = 340.93 K.

TABLE 4. Values of the speed of sound u of saturated liquid HFC32 at different temperatures T and vapour pressure p

T/K	p_σ/MPa	u/(m·s^{-1})
248.20	0.34	832.4[a]
258.13	0.49	781.1[a]
260.80	0.54	767.6[a]
268.22	0.69	726.8[a]
278.12	0.95	670.4[a]
288.31	1.28	612.4[a]
298.18	1.68	553.0
313.19	2.48	458.6
328.25	3.54	356.3
343.29	4.89	235.0

[a] Denotes extrapolated values.

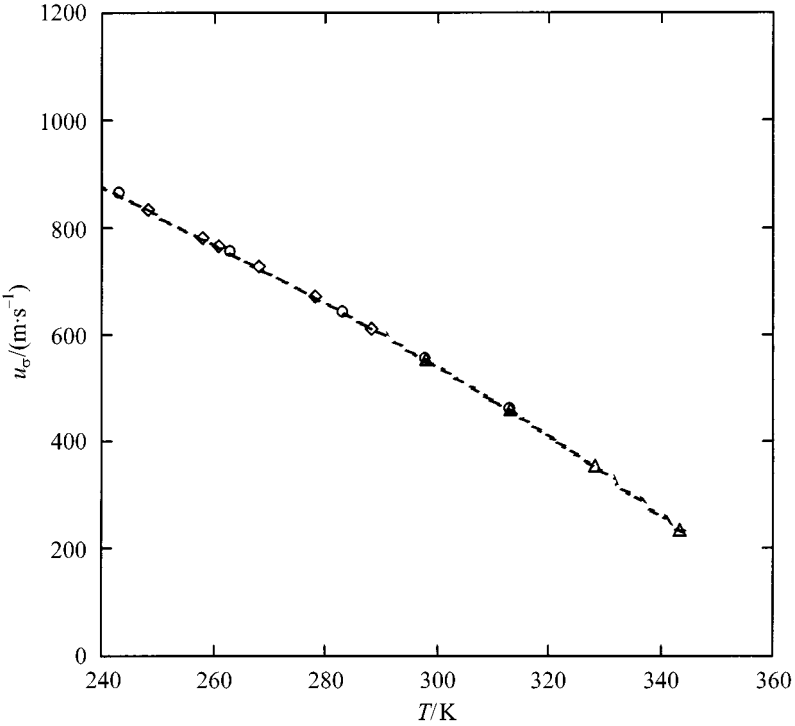

FIGURE 8. Speed of sound u_σ of the saturated liquid HFC32 up to $T = 343$ K. ◇, this work (extrapolated); △, this work (experimental); ○, Takagi (extrapolated); ----, equation (5).

improvement of the International Standard Equation of State for HFC32, which is currently under development.[5,20]

Special thanks are due to Professors C. A. Nieto de Castro and Umesh V. Mardolcar for providing us with the HFC32 sample. P. F. Pires wishes also to thank the Fundação para a Ciência e Technologia for grant No. BD/2522/93-RM.

TABLE 5. Coefficients a_i, b_i, and c_i of equation (6) used to fit the literature density values of HFC32[18]

i	a_i	b_i	c_i
0	$1.69593\cdot10^{+3}$	$-1.06085\cdot10^{+2}$	$-1.19032\cdot10^{+2}$
1	$-6.10446\cdot10^{0}$	$1.63303\cdot10^{0}$	$3.96546\cdot10^{+4}$
2	$8.84873\cdot10^{-3}$	$-3.06884\cdot10^{-3}$	

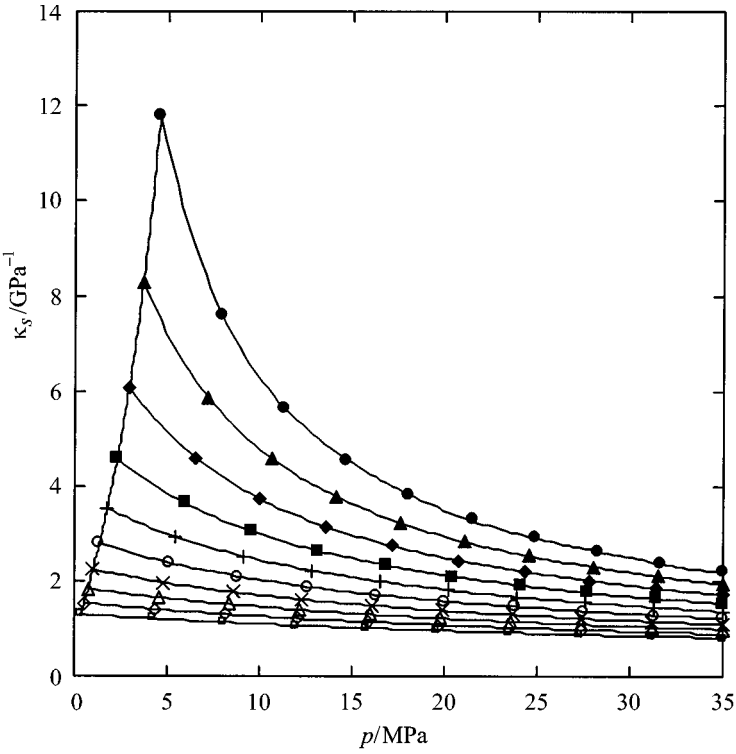

FIGURE 9. Calculated isentropic compressibilities κ_S of liquid HFC32 as a function pressure p at different temperatures T: □, T = 250 K; ◇, T = 260 K; △, T = 270 K; ×, T = 280 K; ○, T = 290 K; +, T = 300 K; ■, T = 310 K; ◆, T = 320 K; ▲, T = 330 K; ●, T = 340 K; ———, saturation curve.

REFERENCES

1. Wuebbles, D. J. *Int. J. Refrig*. **1994,** 17, 7−17.
2. Lunger, B. S.; Geiger, K. A.; Anglin, T. L.; Narayanan, S. *Proceedings of the 1994 International Refrigeration Conference at Purdue*, Purdue University, W. Lafayette, Indiana, U.S.A. **1994,** pp. 25−30.
3. Watanabe, K. *Bulletin of the International Institute of Refrigeration (IIR / IIF)* **1996,** 96.6, 3−14.
4. Kruse, H. *Int. J. Refrig*. **1994,** 17, 149−155.
5. McLinden, M. O.; Lemmon, E. W.; Jacobsen, R. T. *Int. J. Refrig*. **1998,** 21, 322−338.
6. Lísal, M; Vacek, V. *Fluid Phase Equilib*. **1996,** 61−76.
7. Onischenko, V. P.; Zhelezny, V. P.; Vladimirov, B. P. *19th International Congress of Refrigeration*, The Hague, The Netherlands, International Institute of Refrigeration (IIR/IIF). **1995,** IVa, pp. 450−456.
8. Ely, J. F.; Huber, M. L. *Proceedings, ASHRAE Purdue CFC Conference*, Purdue University, W. Lafayette, Indiana, U.S.A. **1990,** pp. 383−392.
9. Ely, J. F. Personal communication.
10. Jelinek, M.; Daltrophe, N.C.; Borde I. *International Conference on Energy Efficiency in Refrigeration and Global Warming Impact*, University of Ghent, Belgium, International Institute of Refrigeration (IIR/IIF). **1993,** pp. 199−206.
11. Takagi, T. *High Temperatures−High Pressures* **1993,** 25, 685−691.

12. Grebenkov, A. J.; Zhelezny, V. P.; Klepatsky, P. M.; Beljaeva, O. V.; Chernjak, Yu.A.; Kotelevsky, Yu.G.; Timofeev, B. D. *Int. J. Thermophysics* **1996,** 17, 535−549.
13. Beljaeva, O. V.; Grebenkov, A.J.; Zajatz, T. A.; Timofeev, B. D. *Bull. of the Acad. of Sciences of Belarus, Phys.-Tech. Science* **1995,** 39, 108−111.
14. Papadakis, E. P. *The Journal of The Acoustical Society of America* **1967,** 42, 1045−1051.
15. Guedes, H. J. R.; Zollweg, J. A. *Int. J. Refrig.* **1992,** 15, 381−385.
16. Muringer, M. J. P.; Trappeniers, N. J.; Biswas, S. N. *Phys. Chem. Liq.* **1985,** 14, 273−296.
17. Nieto de Castro, C. A.; Santos, F. J. V.; Mardolcar, U. V. *19th International Congress of Refrigeration*, The Hague, The Netherlands, International Institute of Refrigeration (IIR/IIF). **1995,** IVa, pp. 436−441.
18. Magee, J. W. *Int. J. Thermophys.* **1996,** 17, 803−822.
19. Sifner, O. *Abstracts of the 13th Symposium on Thermophysical Properties*, Boulder, Colorado, U.S.A. **1997,** p. 332.
20. Craven, R. J. B.; Kilner, J.; Wakeham, W. A. *Abstracts of the 13rd Symposium on Thermophysical Properties*, Boulder, Colorado, U.S.A. **1997,** p. 228.

(Received 2 February 1998; in final form 21 July 1998)

WA98/006